PHYSICAL REVIEW E **92**, 032728 (2015)

Nonlinearities of biopolymer gels increase the range of force transmission

Xinpeng Xu[*] and Samuel A. Safran[†]
Department of Materials and Interfaces, Weizmann Institute of Science, Rehovot 76100, Israel

(Received 21 May 2015; revised manuscript received 26 August 2015; published 29 September 2015)

We present a model of biopolymer gels that includes two types of elastic nonlinearities, stiffening under extension and softening (due to buckling) under compression, to predict the elastic anisotropy induced by both external as well as internal (e.g., due to cell contractility) stresses in biopolymer gels. We show how the stretch-induced anisotropy and the strain-stiffening nonlinearity increase both the amplitude and power-law range of transmission of internal, contractile, cellular forces, and relate this to recent experiments.

DOI: 10.1103/PhysRevE.92.032728 PACS number(s): 87.10.Pq, 62.20.D−, 87.17.Rt

I. INTRODUCTION

Biopolymer hydrogels (e.g., collagen, fibrin, and elastin) comprise crosslinked, semiflexible filaments [1]. They are important constituents of animal tissues [2]. One of the properties that distinguishes these gels [1] from those comprising flexible filaments is their highly non-linear, strain-stiffening response to applied shear stress [3]. For stresses that exceed a critical value (corresponding to small strains about 5%–10% [3,4]), these gels show a power-law stiffening of the elastic modulus with increasing stress, where the elastic modulus in some of these gels increases as the 3/2 power of the applied stress [3]. Recently, collagen-I gels are found to stiffen linearly (instead of 3/2 power) with the applied stress [4]. In contrast to their behavior under stretch, biopolymer gels show nonlinear strain softening upon compression [5,6]. For compressional stresses exceeding a critical value, these gels can can completely lose their resistance to shear stress [5,6]. Such nonlinear shear stiffening and compressive softening can be attributed to the microstructural nonlinearities of the constituent, semiflexible filaments which stiffen under extension and soften (due to buckling) under compression [1,3]. In addition, tensile stresses applied to biopolymer gels can induce anisotropy (due to fiber alignment, for example) in their elasticity [7–9], which has recently been identified as an important mechanism for long-range, cell-cell mechanical signaling [8].

In this paper, we predict the elastic responses of biopolymer gels to stresses in spherical geometries which model the response of the gels to internal stresses such as those induced by symmetrically contractile cells. In earlier theoretical work [10], nonlinear biopolymer gels were modeled, for simplicity, as elastic materials that stiffen under *both* extension or shear as well as under compression. However, biopolymer gels, as mentioned above, are composed of crosslinked semiflexible polymers which, under compression, tend to buckle and lose their resistance to shear, leading to the nonlinear, compressional softening in these systems [5,6]. In contrast, in this paper we propose and analyze a more realistic model of biopolymer gels that *stiffens* under extension or shear and *softens* under compression. This more realistic and unified model results in predictions for force transmission in these systems that differ dramatically from Ref. [10], in which the compressional softening was not taken into account, as well from Refs. [9,11], where the shear stiffening was neglected. Our major predictions are as follows:

(i) A power-law regime in the far field where the displacement scales as R^{-m}, where $m < 2$ is predicted and R is the distance away from the cell center. (Similar scaling was recently found in Refs. [9,11].) This regime originates in the asymmetric responses of biopolymer gels to extension and compression that were not included in Ref. [10].

(ii) The amplitude of the displacement in the far field does not exponentially increase with stiffening nonlinearity as in Ref. [10] but shows a weaker, power-law dependence on the stiffening and the softening nonlinearities. In Refs. [9,11] this amplification of the strain induced by a symmetric source of force (such as a cell) does not occur at all since the stiffening nonlinearity was not included.

These theoretical insights allow us to rationalize recent observations that cells in fibrous ECM can sense mechanical signals over much larger distances compared with linear, elastic, flexible polymer gels [8,9,12,13].

The paper is organized as follows. In Sec. II we present a minimal model of fibrous biopolymer gels that stiffen under extension and soften under compression. We consider the elastic responses of these model biopolymer gels to external, uniaxial tensile stresses. In Sec. III we then show how the nonlinearities of biopolymer gels can increase the range of transmission of internal cellular forces. The paper is concluded in Sec. IV with a few remarks.

II. A MODEL OF BIOPOLYMER GELS

A. Elastic energy density

Biopolymer gels that stiffen upon tensile stresses and soften upon compressive stresses may be modeled by the following elastic energy density in terms of the three principal strain components ϵ_i ($i = 1,2,3$) [14] as

$$f_{\mathrm{e}}(\epsilon_1,\epsilon_2,\epsilon_3) = \sum_{i=1}^{3} w(\epsilon_i) + \frac{K_{\mathrm{os}}}{2}(\epsilon_1 + \epsilon_2 + \epsilon_3)^2, \qquad (1)$$

which includes two separate contributions: the first term characterizes the deformation of the semiflexible polymer chains, and the second term represents the compressibility of the retained water in the gel, with K_{os} being the osmotic bulk modulus describing the osmotic stress when the entire network is isotropically compressed. The physics of water

---

[*] xpxu2010@gmail.com

[†] sam.safran@weizmann.ac.il

flow that govern K_{os} is discussed in Appendix A 2. To phenomenologically model the asymmetric elastic responses of biopolymer gels to extension and compression, we use an energy density $w(\epsilon_i)$ with piecewise continuous form,

$$w(\epsilon_i) = \begin{cases} \mu_0\epsilon_i^2[2(1-\epsilon_i/\epsilon_m)^{-1}-1], & \text{for} \quad \epsilon_i > 0 \\ \rho(\epsilon_i)\mu_0\epsilon_i^2, & \text{for} \quad \epsilon_i < 0, \end{cases} \tag{2}$$

where μ_0 is the linear shear modulus; $\rho(\epsilon_i) = \rho_0 + (1-\rho_0)\Theta(\epsilon_i + \epsilon_m')$ with $0 \leqslant \rho_0 < 1$ characterizing the gel softening due to the polymer buckling [5,6] and $\Theta(x)$ being the Heaviside step function of x. This form of energy density $w(\epsilon_i)$ is directly motivated by the physics of semiflexible polymers [1,9]. More complicated forms are also possible [15], but for simplicity we choose the above piecewise continuous form, which includes the two major microstructural nonlinearities—stiffening under extension and softening under compression. The dimensionless parameters ϵ_m and ϵ_m' account for the critical strain for gel stiffening upon extension and that for gel softening upon compression, respectively [1,9,11]. Note that in the statistical theory of single semiflexible polymers [1], the critical strain ϵ_m' (for buckling) is found to be of the same order of magnitude as the critical strain $\epsilon_m \sim \ell/\ell_p$ for stretch stiffening. However, for a biopolymer gel, a network of crosslinked semiflexible polymers, we expect that ϵ_m' can be much larger or smaller than ϵ_m depending on the mechanical properties of single biopolymers and crosslinkers and the microstructure (e.g., connectivity) of the gel. For example, in fibrin networks the critical strain ϵ_m' for compressive softening can be varied [5,6] so that ϵ_m' can be either larger or smaller than ϵ_m. The relationship is determined by the mechanical properties of fibrin and the network microstructure set by the concentrations of fibrin and the crosslinker [6]. In other networks of crosslinked, semiflexible polymers of hierarchical structure [16], tensile stresses applied to these polymers can stretch out the prefolded molecular structure and thereby increase the resistance of the gel to stretch. This is another type of nonlinear strain stiffening that may occur for strains that exceed a value of ϵ_m which may be (much) larger than the critical strain for compressive softening ϵ_m'. In addition, when water can freely flow out of the compressed gels (see Appendix A 2 for a discussion of gels with zero Poisson ratio), the polymer concentration increases during compression. This effect increases the gel modulus and may partially or completely offset the softening of the gel due to polymer buckling [5,6]; in this case we might expect $\epsilon_m \ll \epsilon_m'$.

B. Strain-stiffening and stretch-induced anisotropy

To demonstrate that our elastic energy corresponds to the properties of biopolymer gels, we first consider their responses to simple shear (with principal strains $\epsilon_1 \approx \gamma/2 > 0$, $\epsilon_2 \approx -\gamma/2 < 0$, and $\epsilon_3 = 0$ for small shear strain $\gamma \ll 1$) [14]. In this case, from the elastic energy density (1) we can calculate the shear stress σ and the differential shear modulus $d\sigma/d\gamma$ as functions of shear strain γ. For infinitesimal shear strain of $\gamma \ll \epsilon_m$, the differential shear modulus is constant and equal to μ_0. As the shear strain increases approaching $\gamma_{\max} \sim 2\epsilon_m$, the shear stress diverges as $\sigma \propto (1-\gamma/2\epsilon_m)^{-2}$ and the differential shear modulus stiffens as $\sigma^{3/2}$. This corresponds to the 3/2-power-law strain stiffening that has been experimentally observed in many biopolymer gels [3] and has been attributed to the inextensibility of single semiflexible polymers [1,3].

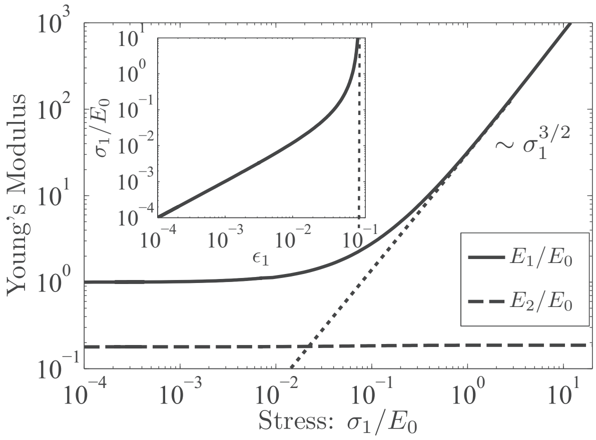

FIG. 1. Stretch-induced anisotropy in Young's moduli for semiflexible polymer gels under external, uniaxial tensile stress σ_1 in the limit of $\epsilon_m' \ll \epsilon_m$. Here $\epsilon_m = 0.1$, $\epsilon_m' = 0$, $\rho_0 = 0.1$; $\nu_0 = 0.49$ and $E_0 = 2\mu_0(1+\nu_0)$. The Young's modulus $E_1 \equiv \partial\sigma_1/\partial\epsilon_1$ is constant $(=E_0)$ for small stress and increases asymptotically to $\sim\sigma_1^{3/2}$ with increasing stress. E_2 is the transverse Young's modulus of the gel under given longitudinal prestress σ_1 is constant $(\approx\rho_0 E_0 \ll E_1)$ in the entire range of stress calculated. Inset: Uniaxial stress vs strain diverges near ϵ_m.

Next, we consider the elastic responses of the modeled biopolymer gels to external uniaxial extensions (along the direction denoted by the subscript 1 with $\epsilon_1 > 0$ and $\epsilon_2 = \epsilon_3 \leqslant 0$ for the non-negative Poisson ratio). In this case, the energy density (1) becomes

$$f_{\text{e}} = \mu_0\left[\epsilon_1^2\left(\frac{2}{1-\epsilon_1/\epsilon_m} - 1\right) + 2\rho(\epsilon_2)\epsilon_2^2\right] + \frac{K_{\text{os}}}{2}(\epsilon_1 + 2\epsilon_2)^2. \tag{3}$$

In the linear limit where $\epsilon_m, \epsilon_m' \to \infty$, the energy density (3) reduces to $f_{\text{e}} = \mu_0(\epsilon_1^2 + 2\rho\epsilon_2^2) + \frac{1}{2}K_{\text{os}}(\epsilon_1 + 2\epsilon_2)^2$, from which we calculated the Young's modulus $E_0 = 2\mu_0(1+\nu_0)$ and the linear Poisson ratio $\nu_0 = K_{\text{os}}/2(K_{\text{os}} + \mu_0)$. However, for biopolymer gels that may stiffen at small extensions, we have $\epsilon_m \ll 1$. Moreover, in biopolymer gels, we expect, as discussed previously, the following three possibilities: $\epsilon_m' \gg \epsilon_m$, $\epsilon_m' \sim \epsilon_m$, and $\epsilon_m' \ll \epsilon_m$. Particularly, in the limit of $\epsilon_m' \ll \epsilon_m$, from the energy density (3) we calculated the longitudinal Young's modulus E_1 (as shown in Fig. 1) that is constant for strain $\epsilon_1 \ll \epsilon_m$ and stiffens as $\sigma^{3/2}$ when the strain ϵ_1 increases, approaching ϵ_m. Such nonlinear elasticity of 3/2-power-law strain stiffening in Young's modulus can also be attributed to the inextensibility of single semiflexible polymers [1,3] as the shear modulus in the case of simple shear. We also calculated the transverse Young's modulus $E_2 = \rho(\epsilon_2)E_0/[1 + \rho(\epsilon_2)\nu_0 - \nu_0]$ (see Fig. 1), which equals the linear Young's modulus E_0 for strain $\epsilon_1 < \epsilon_m'/\nu_0$ (i.e., $\epsilon_2 = -\nu_0\epsilon_1 > -\epsilon_m'$). When $\epsilon_1 > \epsilon_m'/\nu_0$, E_2 becomes smaller than E_0, corresponding to the gel softening that is associated with polymer buckling due to compression in the transverse direction under longitudinal prestress σ_1. That is, the external uniaxial tensile stresses applied to initially *isotropic* biopolymer gels can induce strong *anisotropy* in their elasticity due to the 3/2-power-law strain stiffening in the longitudinal direction and the compressive softening in the transverse direction.

III. LONG-RANGE TRANSMISSION OF INTERNAL CELLULAR FORCES IN SPHERICAL GEOMETRY

Our simple model of biopolymer gels allows us to understand the long-range force transmission of internal contractile forces by cells in the extracellular matrix [8,12,13]. In the simplest case [9,10,17], one can consider the response of gels in spherical geometry to internal forces applied by a spherical, contractile cell [see Fig. 2(a)] [10,12,17]. We characterize the cellular forces by a boundary condition of fixed radial displacement u_0 at the cell-gel interface $R = R_0$ with $u_0 < 0$ for contractile forces [10,17].

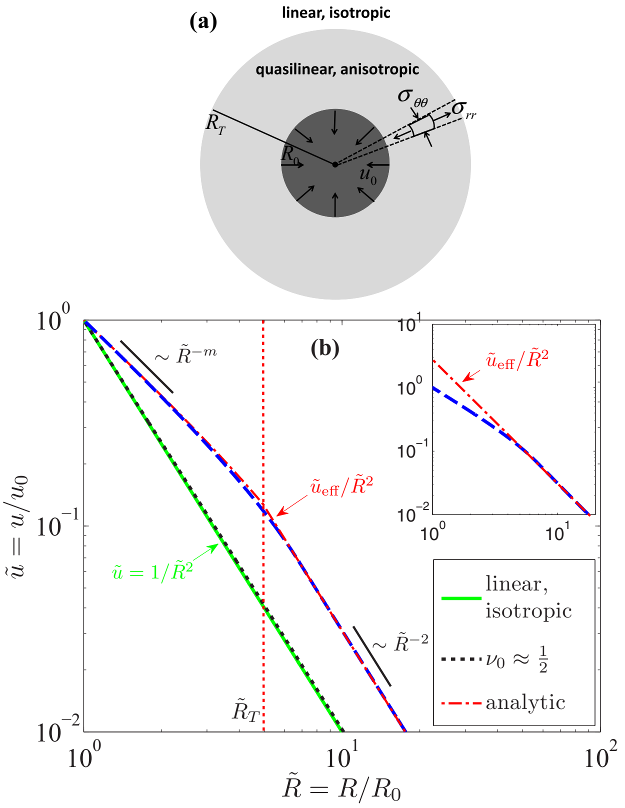

FIG. 2. (Color online) (a) Schematic illustration of a spherical cell exerting contractile force on the extracellular biopolymer gel in the quasilinear limit of $\epsilon_m \to \infty$ and $\epsilon'_m \ll 1$. *Two* regimes separated at $\tilde R = \tilde R_T$ are identified. (b) Numerical solutions of the equilibrium equation (5): normalized displacement vs normalized radius for $\rho_0 = 0.1$. Case 1: $\nu_0 = 0$ (blue dashed line). The decay of displacement can be well approximated by composite materials: a near-field, linear anisotropic material for $1 < \tilde R \ll \tilde R_T$ with a far-field, linear isotropic material for $\tilde R \gg \tilde R_T$. The near-field displacement decays as a power law with exponent $m \approx 1.2$ and the far-field displacement as $\tilde R^{-2}$. The red dash-dotted line is the analytical solution (7) and (9) of linear composite materials. Case 2 – weak compressibility: $\nu_0 = 0.49$ (black dotted line). Its solution is similar to that of linear isotropic materials as shown for comparison (green solid line). Inset: Normalized effective far-field displacement $\tilde u_{\rm eff}$. It shows that the stretch-induced anisotropy in the gel can increase the range of force transmission.

Elastic equilibrium (zero divergence of the stress) applied to our nonlinear gel model predicts extension in the radial direction (strain $\epsilon_{rr} > 0$) and compression in the angular direction (strain $\epsilon_{\theta\theta} < 0$), yielding the equilibrium equation [10,17]:

$$a_0\tilde U - \tilde V + (1 + A\tilde u')^{-3}\left(\tilde U + \frac{3A\tilde u'^2}{\tilde R} + \frac{A^2\tilde u'^3}{\tilde R}\right) = 0, \tag{4}$$

with the boundary conditions $\tilde u(1) = 1$ and $\tilde u(\tilde R \to \infty) = 0$. Here $\tilde U \equiv \tilde u'' + 2\tilde u'/\tilde R$ and $\tilde V = c_0\frac{2\tilde u}{\tilde R^2} - B\frac{\tilde u^2}{2\tilde R^3}\tilde\rho'$; $a_0 \equiv \frac{\nu_0}{2(1-2\nu_0)} - \frac{1}{2}$ and $c_0 \equiv a_0 + \frac{1}{2}(1 + \tilde\rho)$ with $\tilde\rho = \rho_0 + (1 - \rho_0)\Theta(1 - B\tilde u/\tilde R)$ and $\tilde\rho' = (1 - \rho_0)\delta(1 - B\tilde u/\tilde R)$. We have introduced the normalized displacement $\tilde u = u/u_0$, the normalized radius $\tilde R = R/R_0$, and $\tilde u' \equiv d\tilde u/d\tilde R$. The dimensionless parameters $A \equiv -u_0/R_0\epsilon_m$ and $B \equiv -u_0/R_0\epsilon'_m$ ($A, B > 0$ for contractile cells with $u_0 < 0$) characterize the strengths of the nonlinearity of radial stiffening and angular softening, respectively. We now predict the implications of Eq. (4) in several important cases.

A. Force transmission enhanced by stretch-induced anisotropy

We first consider the quasilinear limit of $\epsilon_m \to \infty$ (or $A \to 0$) and $\epsilon'_m \ll 1$ (or $B \gg 1$), in which the nonlinearity of strain stiffening of the gel under extension is negligible but the strain softening under compression can be important. In this quasilinear limit, the gel in the near field (with angular compressive strains $\epsilon_{\theta\theta} < -\epsilon'_m$) responds as a transversely isotropic material [18] due to the asymmetric responses of the biopolymer gels to (radial) extension and (angular) compression [9,11]. In the far field (with $\epsilon_{\theta\theta} > -\epsilon'_m$), the stress decays and the gel behaves like a linear, isotropic material. Therefore we can simply approximate the gel as a linear composite material—a near-field, linear, but transversely isotropic material [18] with a far-field, linear, isotropic material [19] at $\tilde R = \tilde R_T$ where $\epsilon_{\theta\theta}(\tilde R_T) = -\epsilon'_m$.

In the quasilinear limit of $A \to 0$ and $B \gg 1$, the equilibrium equation (4) reduces to

$$\frac{d^2\tilde u}{d\tilde R^2} + \frac{2}{\tilde R}\frac{d\tilde u}{d\tilde R} - G(B,\rho_0,\nu_0)\frac{2\tilde u}{\tilde R^2} = 0, \tag{5}$$

where $G(B,\rho_0,\nu_0) \equiv g(\rho_0,\nu_0) + [1 - g(\rho_0,\nu_0)]\Theta(1 - B\tilde u/\tilde R)$ with $g(\rho_0,\nu_0) \equiv \rho_0 + \nu_0(1 - \rho_0)/(1 - \nu_0)$ $[\rho_0 \leqslant g(\rho_0,\nu_0) \leqslant 1]$ depending sensitively on the Poisson ratio $0 \leqslant \nu_0 < 1/2$ and the parameter $0 \leqslant \rho_0 \leqslant 1$ that characterizes the nonlinearity of *strain softening* of the gel under compression. For a spherical cell adhered to and exerting contractile force on an infinite, biopolymer gel [see Fig. 2(a)], we have the boundary conditions $\tilde u(1) = 1$ and $\tilde u(\tilde R \to \infty) \to 0$ [10,17], the continuity conditions of displacement $\tilde u$, and radial stress component σ_{rr} at $\tilde R = \tilde R_T$, where $\tilde u(\tilde R_T)/\tilde R_T = B^{-1}$.

In the far field, $\tilde R \gg \tilde R_T$, the equilibrium equation (5) reduces to

$$\frac{d^2\tilde u}{d\tilde R^2} + \frac{2}{\tilde R}\frac{d\tilde u}{d\tilde R} - \frac{2\tilde u}{\tilde R^2} = 0, \tag{6}$$

identical to linear isotropic materials [10,17,19]. Its solution is

$$\tilde{u}_{\mathrm{lin}}(\tilde{R}) = \tilde{u}_{\mathrm{eff}}/\tilde{R}^2, \tag{7}$$

as shown in Fig. 2(b). In the near field, $1 < \tilde{R} \ll \tilde{R}_T$, the equilibrium equation (5) reduces to

$$\frac{d^2\tilde{u}}{d\tilde{R}^2} + \frac{2}{\tilde{R}}\frac{d\tilde{u}}{d\tilde{R}} - g(\rho_0,\nu_0)\frac{2\tilde{u}}{\tilde{R}^2} = 0. \tag{8}$$

Note that this equation (8) has the same form of the equilibrium equation as a contractile cell embedded in an intrinsic transversely isotropic material [18]. The solution for the displacement is

$$\tilde{u}_{\mathrm{qlin}}(\tilde{R}) = a\tilde{R}^{m-1} + b\tilde{R}^{-m}, \tag{9}$$

where $m = \frac{1}{2}[\sqrt{1+8g(\rho_0,\nu_0)}+1]$ (with $1 \leqslant m < 2$) and $m = 1$ for $\rho_0 = 0$ (i.e., gels lose stiffness completely upon compression over strain $-\epsilon_m'$).

We match the far-field solution (7) and the near-field solution (9) by the continuity of the displacement and stress at $\tilde{R} = \tilde{R}_T$, where $\tilde{u}_{\mathrm{eff}}/\tilde{R}_T^3 = B^{-1}$; we obtain $a = 1 - b$ and $b = B^{-1}(\frac{m+1}{2m-1})\tilde{R}_T^{m+1}$ with the matching radius $\tilde{R}_T$ satisfying the equation $(\frac{m+1}{2m-1})\tilde{R}_T^{2m-1} - B\tilde{R}_T^{m-2} + (\frac{m-2}{2m-1}) = 0$ and the normalized effective far-field displacement given by $\tilde{u}_{\mathrm{eff}} = B^{-1}\tilde{R}_T^3$, which can be much larger than that of linear, isotropic media for which $\tilde{u}_{\mathrm{eff}} = 1$. In particular, for $m = 1$ we obtain $\tilde{R}_T = \frac{1}{4}(1+\sqrt{1+8B}) > 1$, and if further $B \gg 1$(or $\epsilon_m' \ll 1$), we have $\tilde{R}_T \sim B^{1/2}$ and $\tilde{u}_{\mathrm{eff}} \sim B^{1/2} \gg 1$.

In Fig. 2, we show the solutions of the equilibrium equation (5). The analytic solution (7) and (9) based on linear composite materials fits the numerical solution quite well. In the far field, the gel behaves like a linear, isotropic material with displacement decaying as $\tilde{R}^{-2}$. In the vicinity of the cell (i.e., $\tilde{R} \approx 1$), the near-field displacement $\tilde{u}$ decays as $\tilde{R}^{-m}$, which is longer ranged than the linear, isotropic case. Similar scaling has also been obtained recently in Refs. [9,11,20], but our model also incorporates strain stiffening (see the next section). This longer-ranged force transmission results from the stretch-induced anisotropy in the initially isotropic gels due to the asymmetric responses of the gels to extension and compression [9,11,20].

B. Force transmission enhanced by strain stiffening

We now consider the nonlinear limit of $\epsilon_m \ll 1$ that is more relevant to biopolymer gels which stiffen at small tensile strains $\epsilon \sim \epsilon_m$. In this limit, we must analyze the general equilibrium equation (4). In biopolymer gels, we expect that the relative magnitude of the critical strain ϵ_m' for gel softening to ϵ_m can have values that allow for all the possibilities: $\epsilon_m' \gg \epsilon_m$, $\epsilon_m' \sim \epsilon_m$, and $\epsilon_m' \ll \epsilon_m$. In this section, we explore the importance of the relative magnitudes of ϵ_m' and ϵ_m on the transmission of internal forces in biopolymer gels.

We first consider the force transmission in the cases $\epsilon_m' \gg \epsilon_m$ and $\epsilon_m' \sim \epsilon_m$. Our results in Fig. 3(b) show that the system shows the same behavior in both cases. There are two scaling regimes: one ($\tilde{R} \ll \tilde{R}_*$, with $\tilde{R}_* \equiv R_*/R_0$) where the displacement decreases linearly with $\tilde{R}$ and a far-field regime ($\tilde{R} \gg \tilde{R}_*$), where the displacement decays as $\tilde{R}^{-2}$ as for linear isotropic materials. An asymptotic analysis shows that the new length scale R_* [10] originates in the nonlinear strain-stiffening elasticity of biopolymer gels and is of the order of AR_0 in the highly nonlinear limit of $A \gg 1$. [Note that the scaling law for $\tilde{R}_* \sim A$ found here is completely different from $\tilde{R}_* \sim e^{2A/\sqrt{3}}$ obtained in earlier work [10], in which an isotropically stiffened gel model is employed with compressional stiffening as opposed to softening.]

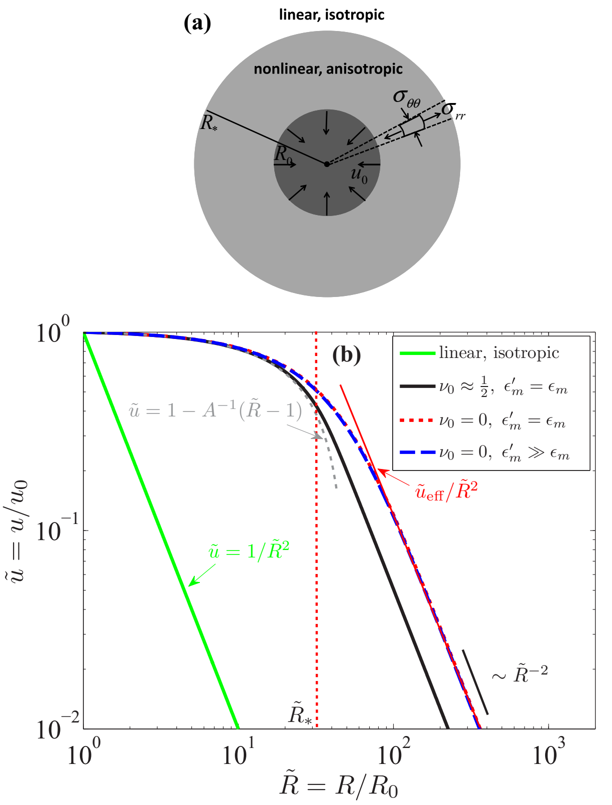

FIG. 3. (Color online) (a) Schematic illustration of a spherical cell exerting contractile force on the extracellular biopolymer gel in the nonlinear limit of $\epsilon_m' \sim \epsilon_m \ll 1$ or $\epsilon_m' \gg \epsilon_m$. *Two* regimes separated by $\tilde{R} = \tilde{R}_*$ are identified. (b) Numerical solutions of the equilibrium equation (4) in the highly nonlinear limit of $A = -u_0/R_0\epsilon_m \gg 1$: normalized displacement vs normalized radius for $A = 50$ and $\rho_0 = 0.1$. Case 1: $\nu_0 = 0$ (red dotted line and blue dashed line). The near-field displacement decays linearly with $\tilde{R}$ (to first order of A^{-1}, gray dotted line). The far-field displacement decays as $\tilde{R}^{-2}$, i.e., as in linear isotropic materials (as shown in the green solid line). Note that the two cases of $\epsilon_m' = \epsilon_m$ and $\epsilon_m' \gg \epsilon_m$ lie on the same line. Case 2 – weak compressibility: $\nu_0 = 0.49$ (black solid line). The solution is qualitatively similar to Case 1 of $\nu_0 = 0$.

In the far field $\tilde{R} \gg \tilde{R}_*$, the stresses decay such that neither the strain-stiffening nonlinearity or the stretch-induced anisotropy are important; the equilibrium equation (4) reduces to Eq. (6) with solution $\tilde{u} = \tilde{u}_{\mathrm{eff}}/\tilde{R}^2$, as shown in Fig. 3(b). $\tilde{u}_{\mathrm{eff}}$ is obtained by matching the nonlinear, near-field solution to the far-field solution and can be much larger than that of linear, isotropic media for which $\tilde{u}_{\mathrm{eff}} = 1$. In the near field $1 < \tilde{R} \ll \tilde{R}_*$ and for strong nonlinearity $A \gg 1$, the stresses applied by the cells on the gels are large and the strain-stiffening nonlinearity and the stretch-induced anisotropy are both important. The near-field displacement is simply expanded as

$$\tilde{u}_{\text{nonlin}} = 1 - A^{-1}(\tilde{R} - 1) \tag{10}$$

to leading order in $1/A$ [see Fig. 3(b)], i.e., the displacement decays almost linearly, much more slowly than that in either linear isotropic media or transversely isotropic media [18]. Additionally, the effects of nonlinearity on the amplitude of force transmission are expressed by the normalized effective far-field displacement $\tilde{u}_{\text{eff}}$, which is obtained by matching the far-field and near-field displacements. Our calculations (see Appendix B 1) show that $\tilde{u}_{\text{eff}} \propto A^2$ (again, completely different from the scaling $\tilde{u}_{\text{eff}} \sim A^{-1}e^{2\sqrt{3}A}$ obtained in earlier work [10]). This means that the nonlinear strain stiffening (quantified by A) of the system can significantly amplify the magnitude of the strain at long distances.

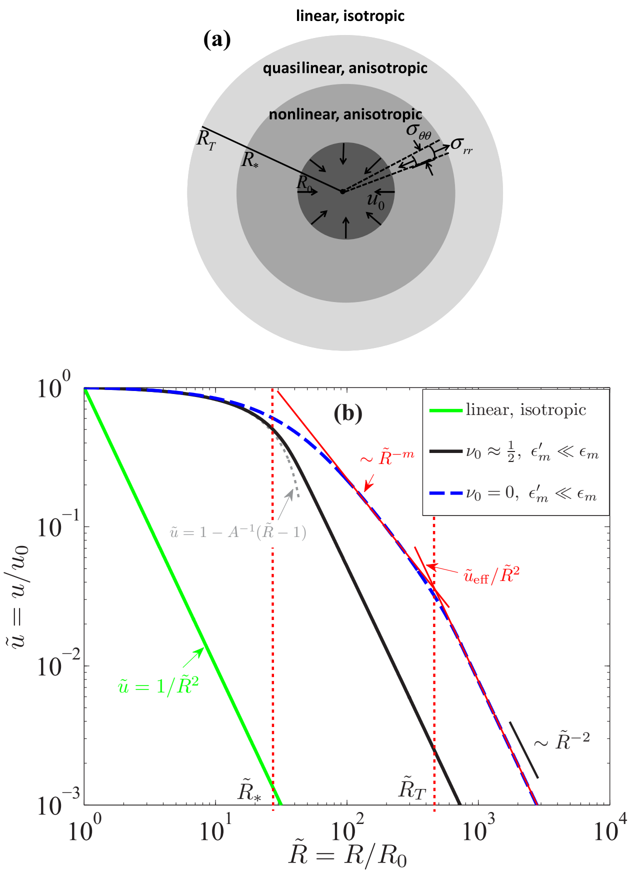

FIG. 4. (Color online) (a) Schematic illustration of a spherical cell exerting contractile force on the extracellular biopolymer gel in the nonlinear limit of $\epsilon'_m \ll \epsilon_m \ll 1$. *Three* regimes separated by $\tilde{R} = \tilde{R}_*$ and $\tilde{R} = \tilde{R}_T$ are identified. (b) Numerical solutions of the equilibrium equation (4) in the highly nonlinear limit of $A = -u_0/R_0\epsilon_m \gg 1$: normalized displacement vs normalized radius for $A = 50$ and $\rho_0 = 0.1$. Case 1: $\nu_0 = 0$ (blue dashed line). The near-field displacement decays linearly with $\tilde{R}$ (to first order of A^{-1}, gray dotted line). In the intermediate quasilinear regime, the displacement decays as in a linear, anisotropic material as $\tilde{R}^{-m}$ with $m \approx 1.2$. The far-field displacement decays as $\tilde{R}^{-2}$, i.e., as in linear isotropic materials (as shown in green solid line). Case 2 – weak compressibility: $\nu_0 = 0.49$ (black solid line). There are only two regimes, as shown in Fig. 3. That is, the effects of stretch-induced anisotropy are important only for *compressible* gels.

We now consider the nonlinear limit of $\epsilon'_m \ll \epsilon_m$ (or $B \gg A$), and in contrast to previous cases we find three distinct scaling regimes for $1 < \tilde{R} \ll \tilde{R}_*$, $\tilde{R}_* \ll \tilde{R} \ll \tilde{R}_T$, and $\tilde{R} \gg \tilde{R}_T$ as shown in Fig. 4, a linearly decaying regime in the near field and the two power-law regimes in the far field. In the limit of zero Poisson ratio $\nu_0 \approx 0$ and strong nonlinearity with $B \gg A \gg 1$, $\rho_0 \approx 0$, an asymptotic analysis shows that $\tilde{R}_* \sim A$ and $\tilde{R}_T/\tilde{R}_* \sim (B/A)^{1/2} \sim (\epsilon_m/\epsilon'_m)^{1/2} \gg 1$.

In the near field $1 < \tilde{R} \ll \tilde{R}_*$ and for strong nonlinearity $A \gg 1$, the displacement decays almost linearly and is approximated by Eq. (10) [see Fig. 4(b)], as in the previous cases of $\epsilon'_m \gg \epsilon_m$ and $\epsilon'_m \sim \epsilon_m$. In the far field, the strain-stiffening nonlinearity becomes unimportant; the equilibrium equation (4) reduces to (5). As discussed in Sec. III A, from Eq. (5) two power-law regimes are identified as shown in Figs. 2(b) and 4(b): (i) $\tilde{R}_* \ll \tilde{R} \ll \tilde{R}_T$ [quasilinear, anisotropic regime, described by Eq. (9)], $\tilde{u}_{\text{qlin}} = a\tilde{R}^{m-1} + b\tilde{R}^{-m}$ with $m = \frac{1}{2}[\sqrt{1 + 8g(\rho_0,\nu_0)} + 1]$ $(1 \leqslant m < 2)$; (ii) $\tilde{R} \gg \tilde{R}_T$ [linear, isotropic regime, described by Eq. (7)], $\tilde{u}_{\text{lin}} = \tilde{u}_{\text{eff}}/\tilde{R}^2$. Again, $\tilde{u}_{\text{eff}}$ is the amplitude of the normalized, effective far-field displacement. That is, in the far field, although the nonlinearity of strain stiffening is negligible, the elastic anisotropy induced by radial tensile stress and angular compressive stress can be important such that the gel responds as a linear composite material [see Figs. 2(b) and 4(b)], in which the range of force transmission is still longer ranged than for the linear isotropic case.

In addition, the effects of near-field nonlinear strain stiffening on the amplitude of force transmission are expressed by the normalized effective far-field displacement $\tilde{u}_{\text{eff}}$, which is obtained by matching the far-field and near-field displacements. Our calculations (see Appendix B 2) show that $\tilde{u}_{\text{eff}} \sim A^{3/2}B^{1/2} \gg 1$ (again, completely different from the scaling $\tilde{u}_{\text{eff}} \sim A^{-1}e^{2\sqrt{3}A}$ obtained in previous work [10] where there was no compressional softening). This means that the nonlinear tensile stiffening (quantified by $A = -u_0/R_0\epsilon_m$) and the nonlinear compressive softening (quantified by $B = -u_0/R_0\epsilon'_m$) of the system can both significantly amplify the magnitude of the strain at long distances.

IV. CONCLUDING REMARKS

In this paper, we have developed a minimal elastic model of fibrous biopolymer gels that stiffen under extension and soften under compression. We predict that external tensile stresses applied to such nonlinear biopolymer gels can induce anisotropy in their elasticity: (i) stiffening in the longitudinal direction where the fibers are stretched, (ii) softening in the transverse direction where the fibers are compressed. We show that the nonlinearities of biopolymer gels can increase the range of transmission of internal cellular forces by (i) introducing a power-law regime with displacement scaling as R^{-m} with $m < 2$ and R being the distance away from the cell center, and (ii) increasing the amplitude of the far-field displacement, which shows power-law dependence on the stiffening and the softening nonlinearities.

Finally, we make a few concluding remarks as follows:

(i) Our minimal model of biopolymer gels may provide a better understanding of a recent experiment [9], which shows that the decay of the displacement (for $R_0 < R < 5R_0$ with

R_0 being the cell radius) induced by a spherical fibroblast cell embedded in a three-dimensional fibrin matrix scales as $R^{-0.5}$. From our calculations, we suggest that it may be the crossover between the near-field (linearly decaying) regime and the far-field (power-law decaying) regimes that results in such an *effective* power between 0 and m $(1 \leqslant m < 2)$. Moreover, our model makes some predictions that could be tested by future experiments: (1) Tensile stresses applied to biopolymer gels can induce strong anisotropy in their elastic moduli, which can be tested by uniaxial stretching experiments. It is also valuable to explore the microscopic parameters (e.g., polymer or crosslinker concentration) that determine the strength of the stretch-induced anisotropy under the same prestress. (2) The stretch-induced anisotropy in hydrogels can increase the transmission range of internal forces, which can be tested in biopolymer gels of various strengths of the stretch-induced anisotropy and for internal forces applied first by localized mechanical probes and eventually by contractile cells.

(ii) Our model for a nonlinear, semiflexible polymer gel unifies two effects: (i) nonlinear strain stiffening (with modulus increasing as the 3/2 power of the applied stress [3]) under extension or shear, and (ii) softening under compression. However, our gel model can be easily extended to biopolymer gels that stiffen at small strains with a modulus that increases with applied stress as a general power law; a linear increase was recently found for collagen I [4], while biopolymers such as fibrin and actin show a 3/2 power law [3]. In these cases, the importance of the strain stiffening on the increase of force transmission is qualitatively similar to what we have predicted. More interestingly, our simple model for gels that unifies their nonlinear response to both stiffening and compression can be generalized to gels which show tensile softening and compressive stiffening [21]. In that case, the radial contractile cellular forces can also induce elastic anisotropy but with *softening* along the radial direction and *stiffening* along the angular direction. The decay of displacement in such transversely anisotropic materials [18] follows a power law R^{-m} with an exponent $m > 2$, which can be seen from the equilibrium equation (5) for $\rho_0 > 1$, characterizing stiffening in the angular directions. That is, in nonlinear gels of tensile softening and compressive stiffening, the stretch-induced anisotropy will *decrease* the range of force transmission in comparison to that of linear isotropic materials.

ACKNOWLEDGMENTS

We thank O. Cohen, K. Dasbiswas, G. A. Holzapfel, P. A. Janmey, F. Jülicher, A. Lesman, J. Notbohm, P. Pincus, Y. Shokef, and V. Vogel for useful discussions. S.A.S. is grateful for support by the Israel Science Foundation and the US–Israel Binational Science Foundation, as well as the Schmidt Minerva Center, the Perlman Family Foundation, and a research grant from the Antonio Viallon family.

APPENDIX A: ELASTIC PROPERTIES OF THE MODELED BIOPOLYMER GELS

In this Appendix, we calculate the properties of the initially isotropic biopolymer gels that are modeled by the elastic energy density (1) in terms of three principal strain components ϵ_i $(i = 1,2,3)$.

1. Stress-strain relations

For the interests of the present work, we consider the special case of $\epsilon_1 > 0$, $\epsilon_2,\epsilon_3 \leqslant 0$. In this case, the elastic energy density (1) becomes

$$f_e(\epsilon_1,\epsilon_2,\epsilon_3) = \mu_0\epsilon_1^2\left(\frac{2}{1-\epsilon_1/\epsilon_m} - 1\right) + \mu_0\rho(\epsilon_2)\epsilon_2^2 + \mu_0\rho(\epsilon_3)\epsilon_3^2 + \frac{K_{os}}{2}(\epsilon_1+\epsilon_2+\epsilon_3)^2, \quad \text{(A1)}$$

where μ_0 is the linear shear modulus; $\rho(\epsilon_i) = \rho_0 + (1-\rho_0)\Theta(\epsilon_i + \epsilon_m')$ with $0 \leqslant \rho_0 < 1$ characterizing the gel softening due to the polymer buckling [5,6] and $\Theta(x)$ being the Heaviside step function of x. From the energy density (A1) we can calculate the three principal stress components $\sigma_i = \partial f_e/\partial\epsilon_i$:

$$\sigma_1 = 2\mu_0\epsilon_1\left[\frac{2-\epsilon_1/\epsilon_m}{(1-\epsilon_1/\epsilon_m)^2} - 1\right] + K_{os}(\epsilon_1+\epsilon_2+\epsilon_3), \quad \text{(A2a)}$$

$$\sigma_2 = \mu_0\left[2\rho(\epsilon_2)\epsilon_2 + \epsilon_2^2\rho'(\epsilon_2)\right] + K_{os}(\epsilon_1+\epsilon_2+\epsilon_3), \quad \text{(A2b)}$$

$$\sigma_3 = \mu_0\left[2\rho(\epsilon_3)\epsilon_3 + \epsilon_3^2\rho'(\epsilon_3)\right] + K_{os}(\epsilon_1+\epsilon_2+\epsilon_3), \quad \text{(A2c)}$$

with $\rho'(\epsilon_i) = d\rho/d\epsilon_i = (1-\rho_0)\delta(\epsilon_i + \epsilon_m')$.

For uniaxial extension (along the direction denoted by the subscript 1) with $\epsilon_1 > 0$, $\epsilon_2 = \epsilon_3 \leqslant 0$ (for non-negative Poisson ratio), the energy density (A1) reduces further to $f_e(\epsilon_1,\epsilon_2)$, as shown in Eq. (3), and the stress components are given by

$$\sigma_1 = 2\mu_0\epsilon_1\left[\frac{2-\epsilon_1/\epsilon_m}{(1-\epsilon_1/\epsilon_m)^2} - 1\right] + K_{os}(\epsilon_1+2\epsilon_2), \quad \text{(A3a)}$$

$$\sigma_2 = \sigma_3 = \mu_0\left[2\rho(\epsilon_2)\epsilon_2 + \epsilon_2^2\rho'(\epsilon_2)\right] + K_{os}(\epsilon_1+2\epsilon_2). \quad \text{(A3b)}$$

Particularly, in the quasilinear limit of $\epsilon_m \to \infty$ and $\epsilon_m' \ll 1$, the stress components (A3) reduce to

$$\sigma_1 = 2\mu_0\epsilon_1 + K_{os}(\epsilon_1+2\epsilon_2), \quad \text{(A4a)}$$

$$\sigma_2 = \sigma_3 = \mu_0\left[2\rho(\epsilon_2)\epsilon_2 + \epsilon_2^2\rho'(\epsilon_2)\right] + K_{os}(\epsilon_1+2\epsilon_2). \quad \text{(A4b)}$$

Furthermore, in the linear limit of $\epsilon_m, \epsilon_m' \to \infty$, the stress components (A4) are further reduced to

$$\sigma_1 = 2\mu_0\epsilon_1 + K_{os}(\epsilon_1+2\epsilon_2), \quad \text{(A5a)}$$

$$\sigma_2 = \sigma_3 = 2\mu_0\epsilon_2 + K_{os}(\epsilon_1+2\epsilon_2). \quad \text{(A5b)}$$

2. Longitudinal Young's modulus and Poisson ratio

For a biopolymer gel under uniaxial tensile stress σ_1^0, we assume homogeneous deformation so that the Young's modulus and Poisson ratio can be calculated by solving the following two coupled algebraic equations:

$$\sigma_1\left(\epsilon_1^0,\epsilon_2^0\right) = \sigma_1^0, \quad \sigma_3 = \sigma_2\left(\epsilon_1^0,\epsilon_2^0\right) = 0. \quad \text{(A6)}$$

From the second equation we calculate $\epsilon_2^0 = \epsilon_2^0(\epsilon_1^0)$ and the Poisson ratio $\nu_{12}(\epsilon_1^0) \equiv -\frac{d\epsilon_2^0}{d\epsilon_1^0}$. (We follow the notation of Poisson ratio in anisotropic materials [7] and define the differential Poisson ratio $\nu_{ij} \equiv -\frac{\partial \epsilon_j}{\partial \epsilon_i}$ for tensile stress applied along i direction and contraction in j direction.) Substituting $\epsilon_2^0(\epsilon_1^0)$ into the first equation of Eq. (A6), we can obtain the stress-strain relation $\sigma_1^0(\epsilon_1^0)$ for uniaxial extension and the Young's modulus $E_1(\epsilon_1^0) \equiv \frac{d\sigma_1^0}{d\epsilon_1^0}$.

We first consider the linear limit of $\epsilon_m, \epsilon_m' \to \infty$. In this case, the stress components are given by Eq. (A5), from which we calculate the Young's modulus $E_1 = E_0$ as

$$E_0 = 2\mu_0(1 + \nu_0), \tag{A7}$$

and the Poisson ratio $\nu_{12} = \nu_0$ with

$$\nu_0 = \frac{K_{\text{os}}}{2(K_{\text{os}} + \mu_0)}. \tag{A8}$$

In Appendix B, we will show that the effects of compressibility on the range of force transmission can be understood in the following two limiting cases [22]:

(i) *Limit of zero Poisson ratio* $\nu_0 = 0$ (or $K_{\text{os}} = 0$). Water can freely flow out of the gel as the polymer network is deformed by applied stresses. In this limit, the elasticity of the gel is purely due to that of the polymer network.

(ii) *Limit of weak compressibility* $\nu_0 \approx 1/2$ (or $K_{\text{os}} \gg \mu_0$). For small time scales, the water does not have time to flow out of the gel but is deformed as the polymer network is distorted. In this limit, the gel can only exhibit weak compressibility with a Poisson ratio very close to 1/2.

For the general nonlinear energy density (3), the stress components are given by Eq. (A3). We calculate the Poisson ratio $\nu_{12} = \nu_0$ (the same with the linear case) and Young's modulus,

$$E_1 = E_0 + \tfrac{12}{5}\mu_0[(1 - \epsilon_1/\epsilon_m)^{-3} - 1]. \tag{A9}$$

Note that near the maximal strain ϵ_m, the uniaxial stress σ_1 in (A3a) diverges as $(1 - \epsilon_1/\epsilon_m)^{-2}$ and the Young's modulus (A9) stiffens as $E_1 \sim (1 - \epsilon_1/\epsilon_m)^{-3}$, i.e., $E_1 \sim \sigma_1^{3/2}$.

3. Transverse Young's modulus and Poisson ratio

To calculate the elastic properties in the transverse direction of the gel under given longitudinal prestress σ_1^0, we apply an infinitesimal stress σ along the transverse (2) direction. In this case, the new equilibrium conditions are given by

$$\sigma_1\left(\epsilon_1^0 + \delta_1, \epsilon_2^0 + \delta_2, \epsilon_2^0 + \delta_3\right) = \sigma_1^0, \tag{A10a}$$

$$\sigma_2\left(\epsilon_1^0 + \delta_1, \epsilon_2^0 + \delta_2, \epsilon_2^0 + \delta_3\right) = \sigma, \tag{A10b}$$

$$\sigma_3\left(\epsilon_1^0 + \delta_1, \epsilon_2^0 + \delta_2, \epsilon_2^0 + \delta_3\right) = 0, \tag{A10c}$$

where ϵ_1^0 and ϵ_2^0 are the strain components calculated from the equilibrium conditions (A6) for uniaxial extension under longitudinal prestress σ_1^0. From Eqs. (A10a) and (A10c), we calculate $\delta_1 = \delta_1(\delta_2; \epsilon_1^0)$ and $\delta_3 = \delta_3(\delta_2; \epsilon_1^0)$, from which we can obtain the differential Poisson ratios $\nu_{21}(\epsilon_1^0) \equiv -\frac{d\delta_1}{d\delta_2}|_{\delta_2=0}$ and $\nu_{23}(\epsilon_1^0) \equiv -\frac{d\delta_3}{d\delta_2}|_{\delta_2=0}$. By substituting $\delta_1(\delta_2; \epsilon_1^0)$ and $\delta_3(\delta_2; \epsilon_1^0)$ into Eq. (A10b) we can obtain $\sigma = \sigma(\delta_2; \epsilon_1^0)$, from which we can calculate the Young's modulus $E_2(\epsilon_1^0) \equiv \frac{d\sigma}{d\delta_2^0}|_{\delta_2=0}$ in the transverse direction.

We first consider the linear limit of $\epsilon_m, \epsilon_m' \to \infty$. In this case, the stress components are given by Eq. (A5), and from Eq. (A10) we calculate the transverse Young's modulus $E_2 = E_0$ and the differential Poisson ratios $\nu_{21} = \nu_{23} = \nu_0$, with E_0 given in Eq. (A7) and ν_0 given in Eq. (A8) being the longitudinal Young's modulus E_1 and Poisson ratio ν_{12} in the linear limit, respectively.

For the general nonlinear energy density (3), the stress components are given by Eq. (A3), and from Eq. (A10) we can numerically calculate the transverse Young's modulus E_2 (see Fig. 1, for example) and the differential Poisson ratios ν_{21}, ν_{23}. Here we do not show the calculations of Poisson ratios, but usually we obtain $\nu_{21} + \nu_{23} \approx 2\nu_{12}$ and $\nu_{21} \neq \nu_{12}$ (different from $\nu_{21} = \nu_{12}$ in intrinsic transversely isotropic materials [18]). That is, although the anisotropy induced in fibrous biopolymer gels by uniaxial tensile stresses has the same *geometric*, hexagonal symmetry as intrinsic transversely isotropic materials [18], they do not have the same *elastic* symmetry. The number of material parameters needed to characterize the anisotropic elasticity is different in the two cases.

APPENDIX B: TRANSMISSION OF INTERNAL CELLULAR FORCES IN SPHERICAL GEOMETRY

In this Appendix, we present our analytic and numerical calculations of the displacements induced in biopolymer gels by internal contractile cellular forces in spherical geometry.

We consider the response of the above modeled biopolymer gels in spherical geometry to internal forces applied by a contractile spherical cell modeled as a contractile force dipole [as schematic in Figs. 2(a), 3(a), and 4(a)] [10,12,17,23]. We characterize the cellular forces by a boundary condition of fixed radial displacement u_0 at the cell-gel interface $R = R_0$ with $u_0 < 0$ for contractile forces [10,17]. We treat the extracellular gel as an infinite and compressible elastic material as described by the energy density (1), which is discussed in Appendix A. Homogeneous deformation is assumed in each small gel element. This situation yields a boundary value problem with inhomogenous deformation in the extracellular gel that depends on the radial coordinate in spherical geometry. Note that in this case the principal directions of strain and stress tensor of each gel element are all along the radial and the two perpendicular angular directions. This significantly simplifies the following calculations.

The equation of mechanical equilibrium is given by [10,17]

$$\frac{d\sigma_{rr}}{dR} + \frac{2}{R}(\sigma_{rr} - \sigma_{\theta\theta}) = 0, \tag{B1}$$

with σ_{rr} and $\sigma_{\theta\theta}$ being the three principal components of the Cauchy stress tensor. The three principal strain components are

$$\epsilon_{rr} = u' \equiv \frac{du}{dR} > 0, \quad \epsilon_{\theta\theta} = \epsilon_{\phi\phi} = \frac{u}{R} < 0. \tag{B2}$$

In this case, from Eqs. (3) and (A3) we obtain the strain energy density and the stress components

$$f_{\mathrm{e}} = \mu_0\left[\epsilon_{rr}^2\left(\frac{2}{1-\epsilon_{rr}/\epsilon_m}-1\right)+2\rho\epsilon_{\theta\theta}^2\right]+\frac{K_{\mathrm{os}}}{2}(\epsilon_{rr}+2\epsilon_{\theta\theta})^2, \tag{B3}$$

$$\sigma_{rr} = 2\mu_0 u'\left[\frac{2-u'/\epsilon_m}{(1-u'/\epsilon_m)^2}-1\right]+K_{\mathrm{os}}(u'+2u/R), \tag{B4a}$$

$$\sigma_{\theta\theta} = \sigma_{\phi\phi} = \mu_0\left[2\rho\frac{u}{R}+\frac{u^2}{R^2}\rho'\right]+K_{\mathrm{os}}(u'+2u/R), \tag{B4b}$$

respectively, with $\rho = \rho_0 + (1-\rho_0)\Theta(u/R+\epsilon_m')$ and $\rho' = (1-\rho_0)\delta(u/R+\epsilon_m')$. Then the equilibrium equation (B1) becomes [10,17]

$$a_0 U - V + (1-u'/\epsilon_m)^{-3}\left(U - \frac{3u'^2}{R\epsilon_m}+\frac{u'^3}{R\epsilon_m^2}\right) = 0, \tag{B5}$$

with the boundary conditions $u(R_0) = u_0$ and $u(R \to \infty) = 0$. Here $U \equiv u'' + 2u'/R$ and $V = c_0\frac{2u}{R^2}+\frac{u^2}{2R^3}\rho'$; $a_0 \equiv \frac{\nu_0}{2(1-2\nu_0)}-\frac{1}{2}$ and $c_0 \equiv a_0 + \frac{1}{2}(1+\rho)$. If we introduce the normalized displacement $\tilde{u} = u/u_0$ and the normalized radius $\tilde{R} = R/R_0$, we obtain the equilibrium equation (4) in its dimensionless form.

Particularly, in the quasilinear limit of $\epsilon_m \to \infty$ and $\epsilon_m' \ll 1$ the equilibrium equation (4) reduces to Eq. (5), whose solutions are discussed in Sec. III A. Two power-law regimes are identified as shown in Fig. 2. Furthermore, in the linear limit of $\epsilon_m, \epsilon_m' \to \infty$, the dimensionless equilibrium equation (4) reduces to Eq. (6), the usual form in linear, isotropic materials [17] whose solution is $\tilde{u} \propto 1/\tilde{R}^2$ to fulfill the natural boundary condition $\tilde{u}(\tilde{R} \to \infty) = 0$.

1. Nonlinear limit: $\epsilon_m' \sim \epsilon_m$ and $\epsilon_m' \gg \epsilon_m$

We now consider the nonlinear limit of $\epsilon_m \ll 1$ that is more relevant to biopolymer gels stiffening at small tensile strains $\epsilon \sim \epsilon_m$. In this nonlinear limit, we must analyze the general equilibrium equation (4). In biopolymer gels, we expect the relative magnitude of the critical strain ϵ_m' for gel softening to ϵ_m can have values that allow for all the possibilities (see discussions in Sec. II B): $\epsilon_m' \gg \epsilon_m$, $\epsilon_m' \sim \epsilon_m$, and $\epsilon_m' \ll \epsilon_m$.

In this Appendix, we study the first two cases: $\epsilon_m' \gg \epsilon_m$ and $\epsilon_m' \sim \epsilon_m$, which show the same behavior as shown in Fig. 3(b). In these cases, two regimes separated by $\tilde{R}_*$ $(=R_*/R_0)$ are identified for the decay of displacement (see Fig. 3). The linearly decaying regime in the near-field and the power-law (with $\tilde{u} \sim \tilde{R}^{-2}$) regime in the far field as in linear isotropic materials.

In the far field where $\tilde{R} \gg \tilde{R}_*$ (A can be large but far-field $\tilde{R} \gg A$), Eq. (4) can be expanded to yield Eq. (6),

$$\frac{d^2\tilde{u}}{d\tilde{R}^2}+\frac{2}{\tilde{R}}\frac{d\tilde{u}}{d\tilde{R}}-\frac{2\tilde{u}}{\tilde{R}^2} = 0,$$

with solution given by Eq. (7) [see Fig. 3(b)],

$$\tilde{u}_{\mathrm{far}}(\tilde{R}) = \tilde{u}_{\mathrm{eff}}/\tilde{R}^2.$$

In the near field where $1 < \tilde{R} \ll \tilde{R}_*$, we consider the special case of strong nonlinearity $A \gg 1$. In this case, we assume that the solution of the equilibrium equation (4) has the form

$$\tilde{u} = 1 + A^{-1}f(\tilde{R}) + A^{-2}g(\tilde{R}) + A^{-3}h(\tilde{R}) \tag{B6}$$

to third order in $A \gg 1$. Since in the limit of strong nonlinearity the denominator $(1 + A\tilde{u}')$ in Eq. (4) is positive and small (close to but not zero, due to the nonlinear strain stiffening of the gel under extension), we can choose $f(\tilde{R}) = -(\tilde{R}-1)$ by noting that $1 - A(\tilde{R}-1)$ solves $1 + A\tilde{u}' = 0$ [10]. By substituting the assumed solution form (B6) and expanding Eq. (4) in powers of $1/A$, we obtain the following equation to order $1/A$:

$$-\frac{2c_0}{\tilde{R}}+\frac{-3\tilde{R}g''(\tilde{R})h'(\tilde{R})+\tilde{R}g'(\tilde{R})h''(\tilde{R})+2g'(\tilde{R})h'(\tilde{R})}{[g'(\tilde{R})]^4} + A\frac{\tilde{R}g''(\tilde{R})-g'(\tilde{R})}{[g'(\tilde{R})]^3} = 0, \tag{B7}$$

with the boundary condition $\tilde{u}(\tilde{R}=1) = 1$. Making the third term of Eq. (B7) (which is order A) vanish yields $g(\tilde{R}) = \frac{1}{2}C(\tilde{R}^2-1)$, where C is a constant that is determined below. Substituting this back into Eq. (B7), we find $h(\tilde{R}) = \frac{2}{3}C^3c_0(\tilde{R}^3-1)+\frac{1}{2}C_1(\tilde{R}^2-1)$. Therefore the near-field solution can be approximated to second order in $1/A$ by

$$\tilde{u}_{\mathrm{near}} = 1 - A^{-1}(\tilde{R}-1)+\tfrac{1}{2}CA^{-2}(\tilde{R}^2-1). \tag{B8}$$

Note that this solution indeed makes the denominator $(1 + A\tilde{u}')$ in Eq. (4) positive and small (close to but not zero) if the coefficient C is positive and not large. In Fig. 3(b), we have shown that for the case of strong nonlinearity with $A \gg 1$, this solution (B8) indeed provides a very good approximation to the near-field solution (with C fitted to be about 0.5).

Finally, for the case of strong nonlinearity with $A \gg 1$, we match the far-field solution (7) and the near-field solution (B8) to first order in $1/A$ or Eq. (10), $\tilde{u}_{\mathrm{near}} = 1 - A^{-1}(\tilde{R}-1)$, by the continuity of the displacement and the radial stress component at the matching radius $\tilde{R}_*$,

$$\frac{\tilde{u}_{\mathrm{eff}}}{\tilde{R}_*^2} = 1 - A^{-1}(\tilde{R}_*-1), \qquad \frac{2\tilde{u}_{\mathrm{eff}}}{\tilde{R}_*^3} = A^{-1}, \tag{B9}$$

from which we obtain the matching radius

$$\tilde{R}_* \propto A, \tag{B10}$$

and the normalized effective far-field displacement

$$\tilde{u}_{\mathrm{eff}} \propto A^2. \tag{B11}$$

These results have been verified by our numerical calculations as shown in Fig. 5. This means that the nonlinear strain stiffening (quantified by $A = -u_0/R_0\epsilon_m$) of the elastic biopolymer gels can significantly magnify the magnitude of the strain at long distances.

2. Nonlinear limit: $\epsilon_m' \ll \epsilon_m$

Now we examine the nonlinear limit where $\epsilon_m' \ll \epsilon_m \ll 1$ (or $B \gg A$). In this case, three regimes separated by $\tilde{R}_*$ and $\tilde{R}_T$ are identified as shown in Fig. 4: the linearly decaying regime in the near field and the two power-law regimes in the far field.

In the near field where $1 < \tilde{R} \ll \tilde{R}_*$, the previous arguments for the nonlinear cases of $\epsilon_m' \sim \epsilon_m$ and $\epsilon_m' \gg \epsilon_m$ also

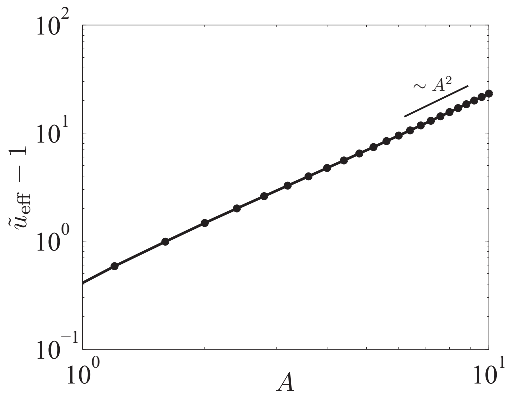

FIG. 5. Normalized effective far-field displacement $\tilde{u}_{\mathrm{eff}}$ vs nonlinearity parameter $A \equiv -u_0/R_0\epsilon_m$ in the nonlinear limit of $\epsilon'_m \sim \epsilon_m \ll 1$. Here lines are plotted only for guidance.

apply here. The near-field solution can be approximated by Eq. (B8) to first order in $1/A$ or Eq. (10):

$$\tilde{u}_{\mathrm{nonlin}}(\tilde{R}) = 1 - A^{-1}(\tilde{R} - 1).$$

In the far field where $\tilde{R} \gg \tilde{R}_*$, the equilibrium equation (4) reduces to Eq. (5) from which two power-law regimes can be identified [see Fig. 4(b)], as discussed in Sec. III A.

(i) For $\tilde{R} \gg \tilde{R}_T$, the solution is given by Eq. (7):

$$\tilde{u}_{\mathrm{lin}}(\tilde{R}) = \tilde{u}_{\mathrm{eff}}/\tilde{R}^2.$$

(ii) For $\tilde{R}_* \ll \tilde{R} \ll \tilde{R}_T$, the solution is given by Eq. (9):

$$\tilde{u}_{\mathrm{qlin}}(\tilde{R}) = a\tilde{R}^{m-1} + b\tilde{R}^{-m},$$

where $m = \frac{1}{2}[\sqrt{1 + 8g(\rho_0,\nu_0)} + 1]$ (with $1 \leqslant m < 2$) and $m = 1$ for $\rho_0 = 0$ (i.e., gels lose stiffness completely upon compression over strain $-\epsilon'_m$).

We match the two far-field solutions (7) and (9) and the near-field solution (10) by the continuity of the displacement and the radial stress component σ_{rr} at the two matching radii $\tilde{R}_*$ and $\tilde{R}_T$ where $\tilde{u}(\tilde{R}_T)/\tilde{R}_T = B^{-1}$. We obtain a system of algebraic equations as follows:

$$\begin{aligned} \tilde{u}_{\mathrm{eff}}\tilde{R}_T^{-3} &= B^{-1}, \\ \tilde{u}_{\mathrm{eff}}\tilde{R}_T^{-2} &= a\tilde{R}_T^{m-1} + b\tilde{R}_T^{-m}, \\ -2\tilde{u}_{\mathrm{eff}}\tilde{R}_T^{-3} &= a(m-1)\tilde{R}_T^{m-2} - bm\tilde{R}_T^{-m-1}, \\ 1 - A^{-1}(\tilde{R}_* - 1) &= a\tilde{R}_*^{m-1} + b\tilde{R}_*^{-m}, \\ -A^{-1} &= a(m-1)\tilde{R}_*^{m-2} - bm\tilde{R}_*^{-m-1}. \end{aligned} \tag{B12}$$

Particularly, for the simple case $m = 1$, we can solve Eq. (B12) and obtain

$$\tilde{R}_* = \frac{1 + A}{2 - (A/2B)^{1/2}}, \quad \frac{\tilde{R}_T}{\tilde{R}_*} = (B/2A)^{1/2}, \tag{B13}$$

and the normalized effective far-field displacement

$$\tilde{u}_{\mathrm{eff}} = (2A)^{-3/2}B^{1/2}\tilde{R}_*^3. \tag{B14}$$

Since $\epsilon'_m \ll \epsilon_m \ll 1$ (or $B \gg A \gg 1$), we obtain the matching radii

$$\tilde{R}_* \sim A, \tag{B15a}$$

$$\tilde{R}_T/\tilde{R}_* \sim (B/A)^{1/2} \gg 1, \tag{B15b}$$

and the normalized effective far-field displacement

$$\tilde{u}_{\mathrm{eff}} \sim A^{3/2}B^{1/2} \gg 1. \tag{B16}$$

This means that the nonlinear tensile stiffening (quantified by $A = -u_0/R_0\epsilon_m$) and the nonlinear compressive stiffening of the elastic biopolymer gels can both significantly magnify the magnitude of the strain at long distances.

---

[1] C. P. Broedersz and F. C. MacKintosh, Rev. Mod. Phys. **86**, 995 (2014).

[2] B. Alberts, A. Johnson, J. Lewis, M. Raff, K. Roberts, and P. Walter, *Molecular Biology of the Cell*, 5th ed. (Taylor & Francis, London, 2007).

[3] M. L. Gardel, J. H. Shin, F. C. MacKintosh, L. Mahadevan, P. Matsudaira, and D. A. Weitz, Science **304**, 1301 (2004); C. Storm, J. J. Pastore, F. C. MacKintosh, T. C. Lubensky, and P. A. Janmey, Nature (London) **435**, 191 (2005).

[4] A. J. Licup, S. Münster, A. Sharma, M. Sheinman, L. M. Jawerth, B. Fabry, D. A. Weitz, and F. C. MacKintosh, arXiv:1503.00924.

[5] O. V. Kim, R. I. Litvinov, J. W. Weisel, and M. S. Alber, Biomaterials **35**, 6739 (2014).

[6] O. V. Kim, X. Liang, R. I. Litvinov, J. W. Weisel, M. S. Alber, and P. K. Purohit, Biomech. Model. Mechanobiol. (2015).

[7] D. Vader, A. Kabla, D. Weitz, and L. Mahadevan, PLoS One **4**, e5902 (2009).

[8] X. Ma, M. E. Schickel, M. D. Stevenson, A. L. Sarang-Sieminski, K. J. Gooch, S. N. Ghadiali, and R. T. Hart, Biophys. J. **104**, 1410 (2013); M. S. Rudnicki, H. A. Cirka, M. Aghvami, E. A. Sander, Q. Wen, and K. L. Billiar, *ibid.* **105**, 11 (2013); A. S. Abhilash, B. M. Baker, B. Trappmann, C. S. Chen, and V. B. Shenoy, *ibid.* **107**, 1829 (2014); H. Wang, A. S. Abhilash, C. S. Chen, R. G. Wells, and V. B. Shenoy, *ibid.* **107**, 2592 (2014).

[9] J. Notbohm, A. Lesman, P. Rosakis, D. A. Tirrell, and G. Ravichandran, J. R. Soc., Interface **12**, 20150320 (2015).

[10] Y. Shokef and S. A. Safran, Phys. Rev. Lett. **108**, 178103 (2012); **109**, 169901(E) (2012).

[11] P. Rosakis, J. Notbohm, and G. Ravichandran, arXiv:1412.2612.

[12] U. S. Schwarz and S. A. Safran, Rev. Mod. Phys. **85**, 1327 (2013).

[13] J. P. Winer, S. Oake, and P. A. Janmey, PloS One **4**, e6382 (2009).

[14] G. A. Holzapfel, *Nonlinear Solid Mechanics* (Wiley, Chichester, 2000); A. F. Bower, *Appl. Mech. Solids* (CRC Press, Boca Raton, FL, 2009).

[15] E. M. Huisman, C. Storm, and G. T. Barkema, Phys. Rev. E **78**, 051801 (2008).

[16] A. E. Brown, R. I. Litvinov, D. E. Discher, P. K. Purohit, and J. W. Weisel, Science **325**, 741 (2009).

[17] D. Ben-Yaakov, R. Golkov, Y. Shokef, and S. A. Safran, Soft Matter **11**, 1412 (2015).

[18] S. G. Lekhnitskii, *Theory of Elasticity of an Anisotropic Body* (Mir Publishers, Moscow, 1981).

[19] L. Landau and E. M. Lifshitz, *Theory of Elasticity* (Pergamon Press, Oxford, 1986).

[20] P. Ronceray, C. Broedersz, and M. Lenz, arXiv:1507.05873.

[21] K. Pogoda, L. Chin, P. C. Georges, F. J. Byfield, R. Bucki, R. Kim, M. Weaver, R. G. Wells, C. Marcinkiewicz, and P. A. Janmey, New J. Phys. **16**, 075002 (2014).

[22] J. Yuval and S. A. Safran, Phys. Rev. E **87**, 042703 (2013).

[23] U. S. Schwarz and S. A. Safran, Phys. Rev. Lett. **88**, 048102 (2002).